3 Results

3.1 *In vitro* protein synthesis: Optimization of RTS 100 and RTS 500 systems

3.1.1 GFP as reporter protein and quality criteria for judgment of the protein expression level

We used the green fluorescent protein (GFP) as a reporter protein. GFP is a fluorescent molecule of 238 amino acids and discovered for the first time in the jellyfish *Aequorea victoria*. The protein has a unique structure consisting of an 11-strands β-barrel (β-Can) forming a cylinder with a central and almost coaxial α-helix that forms autocatalytically a fluorophore from the tri-peptide sequence Ser65-Tyr66-Gly67 (Ormo et al., 1996; Yang et al., 1996). Once folded the fluorescent protein is very stable and *e.g.* resists heat (up to 65°C) and tolerates a pH up to 11; for review see (Tsien, 1998).

Since the GFP band hardly overlaps with any of the S30 extract bands in an SDS gel, the total amount of the protein synthesized *in vitro* can be easily assessed by densitometer analysis of the GFP band, in comparison with defined amounts of purified reference GFP added to the same gel. Furthermore, one stable S30 band was exploited to normalize the input variations of the S30 reaction mixture per lane (Figure 7a). With GFP we can determine not only the total yield, but also the active amount of the synthesized protein by measuring its fluorescence in a native gel. After the synthesis is finished, its fluorophore has to be folded properly, which is a criterion for activity detected by fluorescence of GFP using ultraviolet-light (UV) excitation. GFP can emit green light even after electrophoresis under non-denaturing conditions (i.e. in the absence of SDS; Figure 7b), which allows the estimation of the amount of active molecules by using a commercially available recombinant GFP (rGFP, Roche) that was *in vivo* expressed and assumed to be 100% active as reference.

We can calculate the active fraction of synthesized GFP from both the amount of active GFP and the total amount synthesized (SDS gel). According to this procedure the active fraction was not higher than 30% in the experiment

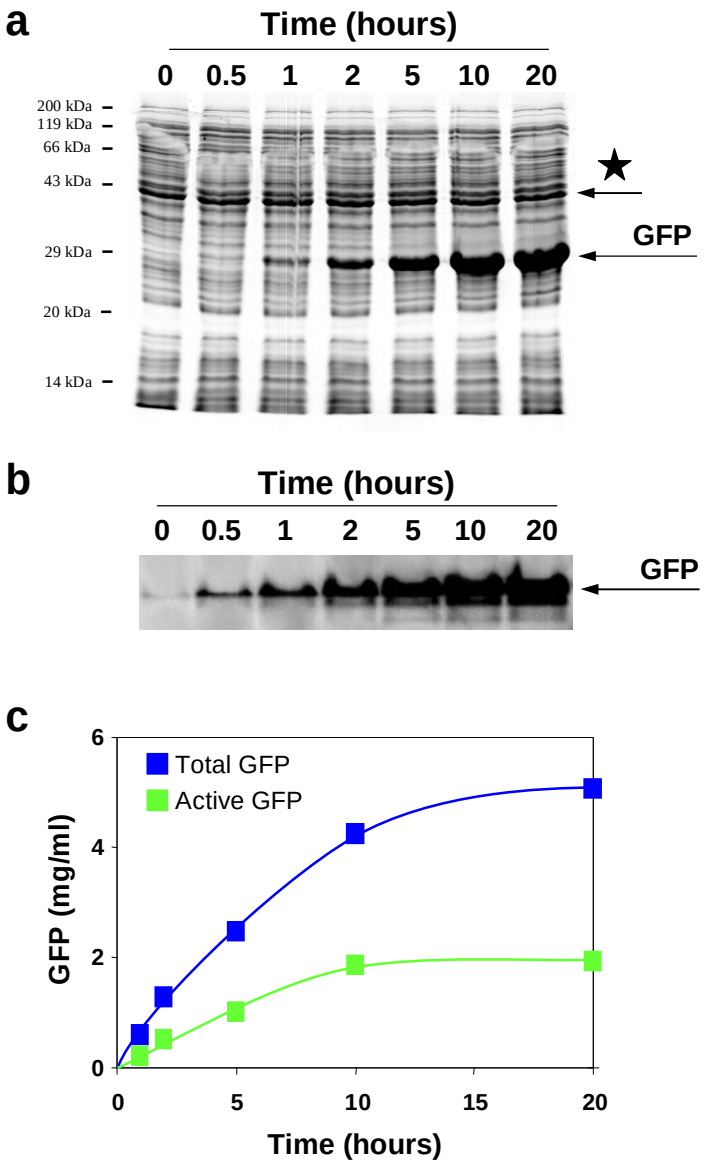

Figure 7: Quality criteria for the determination of synthesized reporter protein GFP. (**A**) one aliquot from kinetics of the GFP synthesis in the RTS 500 reaction mix was applied on SDS-PAGE. Star, S30 band used to normalize input per lane. (**B**) a sister aliquot was applied to a native PAGE and the fluorescence of GFP monitored. (**C**) GFP synthesis in the course of a 20 h incubation. Blue squares, total synthesis of GFP (SDS-PAGE); green squares, active GFP (native-PAGE).

shown in Figure 7c, and (50±20)% on average (see for example Dinos et al., 2004) and Figure 7b. With the help of these quality criteria we aimed to improve the GFP active fraction up to 100%.

3.1.2 Synchronizing the reactions of transcription and translation

In the *E. coli* cell the endogenous RNA polymerase synthesizes about 60 nts of mRNA per second. The ribosome produces about 20 amino acids per

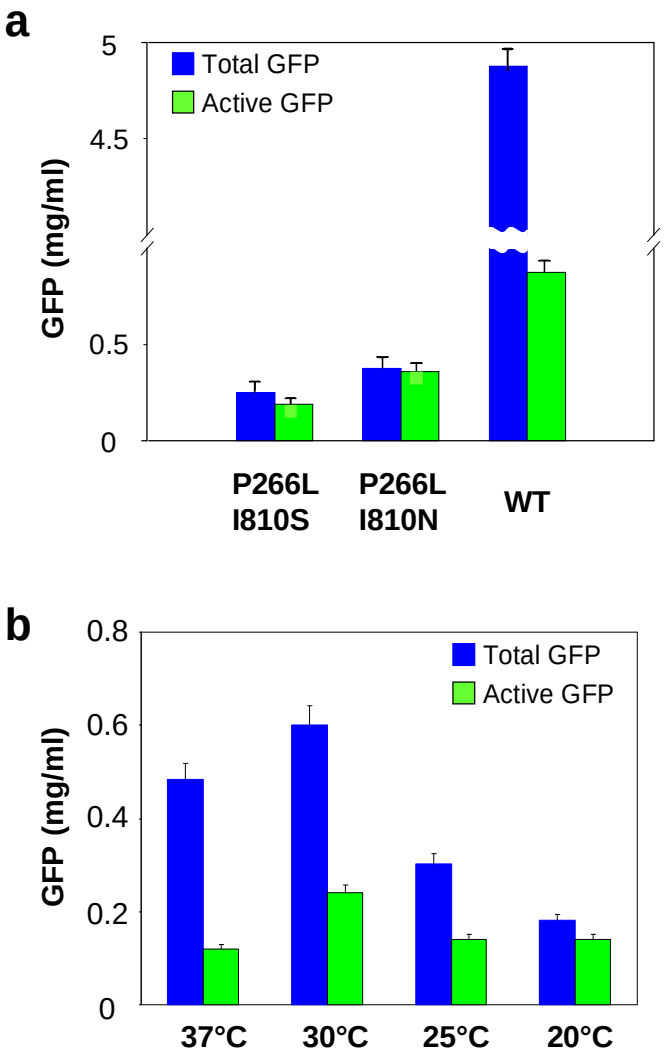

Figure 8: Total and active GFP synthesized at various conditions. Blue bars, total GFP synthesis; green bars, active GFP. **(A)**, GFP synthesized after 20 h at 30 °C of incubation in the presence of mutant T7 transcriptases and our reaction-mix preparation (semi-continuous system; 1 ml reaction volume; the unusually low active fraction of almost 20% might be due to our preparation procedure of the S30 lysate). **(B)**, GFP synthesis after 12 h in the RTS 100 (batch system; 10 µl reaction volume, wild-type T7 polymerase) at various incubation temperatures.

second, what means that these both macromolecules move on the mRNA with the same rate (20 amino acids is equal to 60 nts on mRNA). This coupled movement

prevents the generation of any secondary structure on mRNA, since the first ribosome is just behind the polymerase and thus leaves no significant gap to the forerunning polymerase. In standard cell-free systems the original RNA polymerase is replaced by the 6- to 8-fold faster T7 polymerase from the T7 phage (T7 RNAP). Therefore, the fast transcription generates an increasing gap between the polymerase and the first following ribosome giving chance to the formation of stem-loops, which hinder the translational movement of ribosomes.

Isolation of T7 RNAP have been reported which are slow and have a high processivity (Bonner et al., 1994; Makarova et al., 1995). We received plasmids containing the genes of some these mutants from Dr. Dreyfus in Paris including the double-mutant P266L/I810S being up to six-times slower than the wild-type T7 polymerase. The latter mutation slows the transcriptase, and the former improves the processivity (Guillerez et al., 2005; Makarova et al., 1995). Another mutant is P266L/I810N being 2.5 times slower, both were used in our *in vitro* transcription-translation system.

The SDS PAGE analysis of the synthesized GFP in the system containing one or the other T7 polymerase mutant was disappointing: the yield of GFP was very low in the presence of the mutant P266L/I810N and almost undetectable in the case of the P266L/I810S mutant. However, the determination of the active amount of GFP in the native-PAGE analysis revealed that the low amount of synthesized GFP was fully active (summarized in Figure 8a). It follows that in principle our expectation was fulfilled.

Another way of slowing down the T7 RNAP is by lowering the incubation temperature. A beneficial effect can be expected, if the reduced temperature slows down the translational rate to a lesser extent than the transcriptional rate, thus also improving the coupling of transcription and translation. Credit to this assumption is provided by a previous report saying that in a similar case the T7-transcribed rRNA fraction assembled into active ribosomes was improved dramatically (from 15 to 60%, respectively) by lowering the growth temperature from 37°C to 25°C, which indicates that the rate of T7 RNAP goes down faster than the assembly rate (Lewicki et al., 1993).

GFP was synthesized at various temperatures (37°C, 30°C, 25°C and 20°C; 12 h incubation) under RTS 100 conditions in order to examine the effect on

both total protein synthesis and active GFP. The results are summarized in Figure 8b, from which it is clear that the total yield is two to three times reduced, but that the active fraction approaches 100% at 20°C in a batch system. In order to test whether the beneficial effects of lowering the incubation temperature from 30 to 20°C is not restricted to the protein GFP and might be valid for other proteins as well, we performed a control experiment with luciferase. The results (Table 1) show that the specific activity of luciferase (activity per mass unit) is increased two times similar to the effects seen with GFP in Figure 8a and Figure 8b.

	[^{35}S]-Met incorporation (pixels)	**Luciferase activity (lumino units)**	**Specific activity (lumino units / [^{35}S]-Met pixels) x 1000**	**Relative activity (%)**
20°C	299,899 ± 10%	47,175± 2%	157.3	**100**
30°C	1,103,493 ± 3%	94,515 ± 2%	85.7	**54**

Table 1: Luciferase expression in a coupled transcription-translation system at 20°C and 30°C. [^{35}S]-Met incorporation was determined by the pixels of the radioactivity band corresponding to luciferase in a 15% PAGE and visualized by a PhosphorImager, and the luciferase activity as described by the manufacturer (Promega). For details see Material and Methods. GFP expression was determined as a control and showed about the same strong expression as seen in Figure 8b.

3.1.3 Increasing the total protein yield in RTS 100/500

Two additional parameters might influence the yield of the synthesized protein: the stability of mRNA and the availability of building units such as NTP's and amino acids. These parameters are analyzed in this section. The half-lives of mRNAs in the bacterial cell at 37°C are one minute (most labile mRNAs) to 7.5 minutes (ribosomal proteins mRNA, (Mohanty and Kushner, 1999), with two to three minutes on average for most of the mRNAs in *E. coli* (Selinger et al., 2003).

To test whether an increased mRNA stability improves the protein yield, we exploited the enormous stability of the ribosomal precursor RNA due to the long complementary sequences flanking the mature rRNA (Liiv et al., 1996; right panel in Figure 9a). Our colleague Jaanus Remme (Tartu, Estonia) constructed a GFP-mRNA that is flanked by the highly conserved sequences enclosing the 23S rRNA

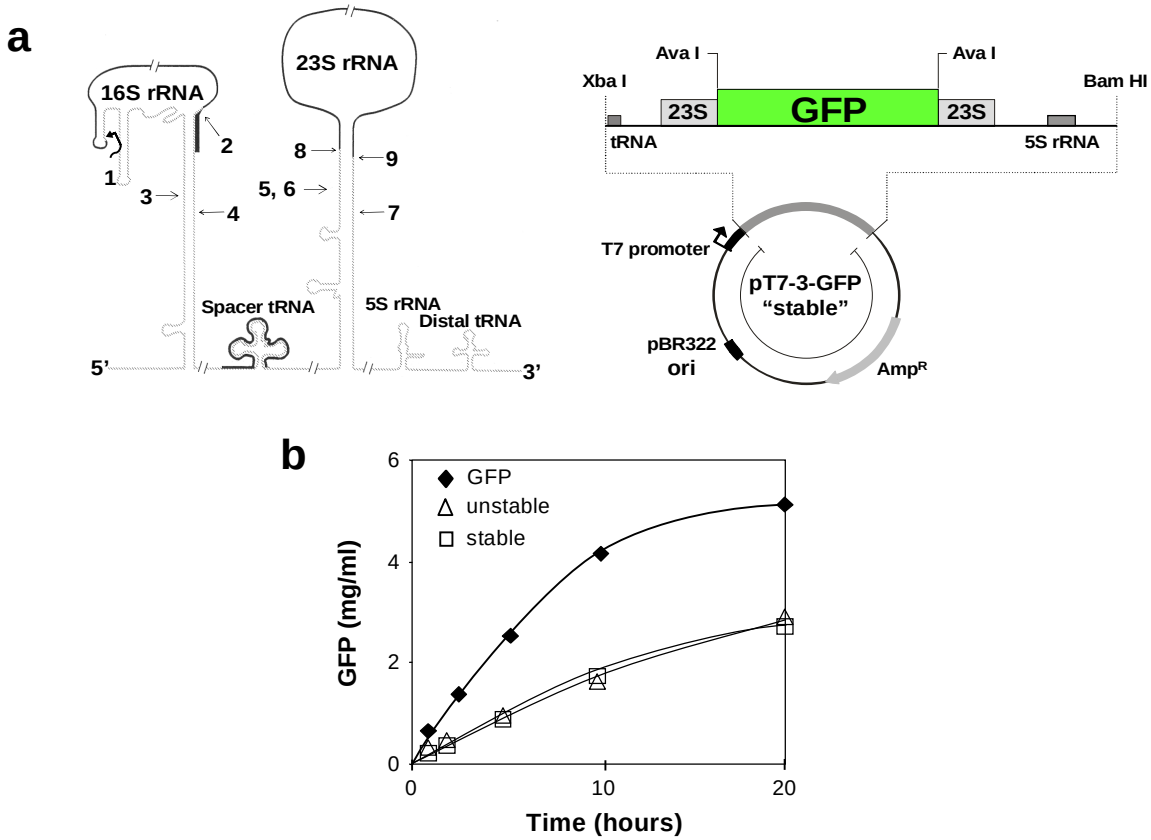

Figure 9: Various mRNA constructs in the coupled transcription-translation system. (**A**) left panel, stability elements of rRNA genes. Scheme of an *rrn* operon and major processing steps of the 16S and 23S rRNA. The drawing is not to scale. Primary processing cleavages by RNase III (3, 4, 5, 6, and 7), and secondary processing to produce the mature termini of 16S rRNA (1, 5' end; 2, 3' end) and 23S rRNA (8, 5' end; 9, 3' end). Solid lines indicate mature RNAs; modified (Srivastava and Schlessinger, 1990). A right panel, map of a plasmid used for mRNA stability test; derivative of a vector that contained a fragment of the *rrnB* operon including intergenic spacers. GFP was incorporated into the 23S rRNA sequence at *Ava*I cleavage sites into a position between nucleotides 250 and 2773 (*E. coli* numbering, starting from 5'end of 23S rRNA). Restriction sites and *rrnB* operon elements are indicated. (**B**) total GFP synthesis from different plasmid-DNA constructs (semi-continuous system; reaction volume 1 ml). Rectangles, GFP-mRNA flanked by the 23S rRNA stability elements ("stable"); triangles, same as rectangles but with destroyed stability elements ("unstable"); closed diamonds, standard expression vector for GFP synthesis ("GFP"). See text for further explanations.

and forms a strong base-paired stem resulting in a pseudo-circularization of the mRNA similar to that of the precursor rRNA ("stable" GFP-mRNA, left panel in Figure 9a). We expected a prolonged mRNA half-life, since the endo RNase E prefers substrates with unpaired 5' ends and the exo- PNPase and RNase II are specific for single stranded RNAs (Carpousis and Dreyfus, 2004). As a control we used the same mRNA except that the mutation in the 5' flanking region disrupts the complementarity and thus pseudo-circularized mRNA fails to be produced

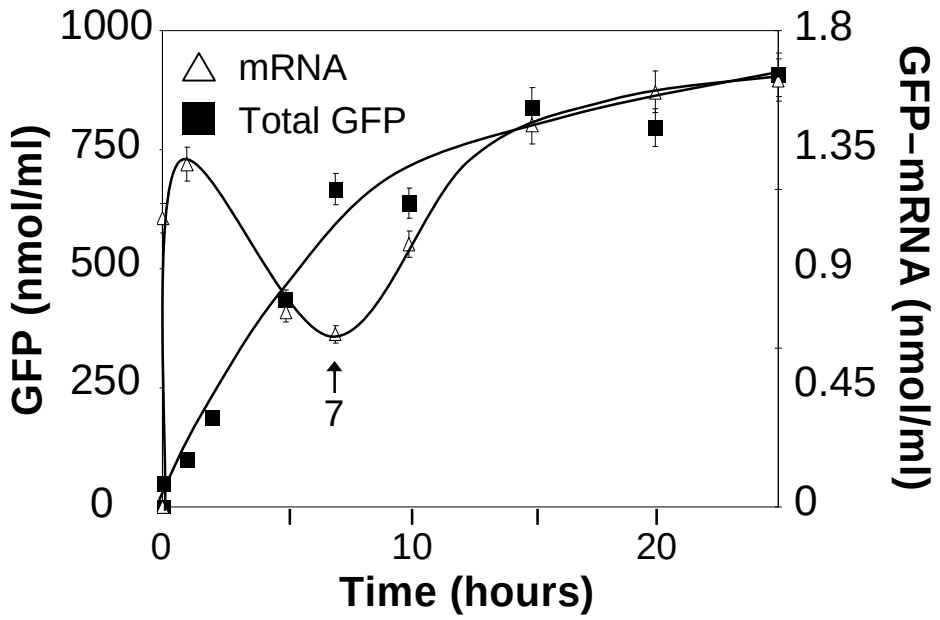

Figure 10: Synthesis of GFP-mRNA and GFP in the RTS 500 system (1 ml reaction). Open triangles, amounts of GFP-mRNA synthesized and determined by Northern blotting; closed squares, total GFP synthesis.

("unstable" GFP-mRNA). The latter (in contrast to the former) has been shown to be resistant against RNase III cleavage *in vitro* that is specific for secondary structures revealing that no secondary structure has been formed (Liiv and Remme, 2004). With both constructs, however, we observed levels of GFP production that were two times less than from our usual construct for GFP expression (Figure 9b). Due to the low yield of GFP synthesis we did not pursue further the question whether indeed the "stable" construct provided a more stable mRNA.

To test directly whether the mRNA stability in the coupled transcription-translation system is an issue, we determined the amount of GFP mRNA present during 25 h synthesis at 30°C *via* Northern blot hybridization and simultaneously the amount of synthesized GFP. The kinetics is shown in Figure 10. The rate of mRNA synthesis peaks after one hour demonstrating the speed of T7 RNAP, and then decreases, whereas the rate of GFP synthesis is maximal until the 7th hour of incubation. When the GFP synthesis ceases after the 7th hour, the amount of GFP-mRNA recovers again. These observations clearly indicate that NTPs are not

limiting the reaction of transcription, which altogether confirms that neither synthesis of mRNA nor its half-life are limiting factors for protein synthesis in the bacterial cell-free system.

However, a shortage of amino acids could be the reason for a reduction of protein synthesis, since according to Swartz and colleagues some amino acids are

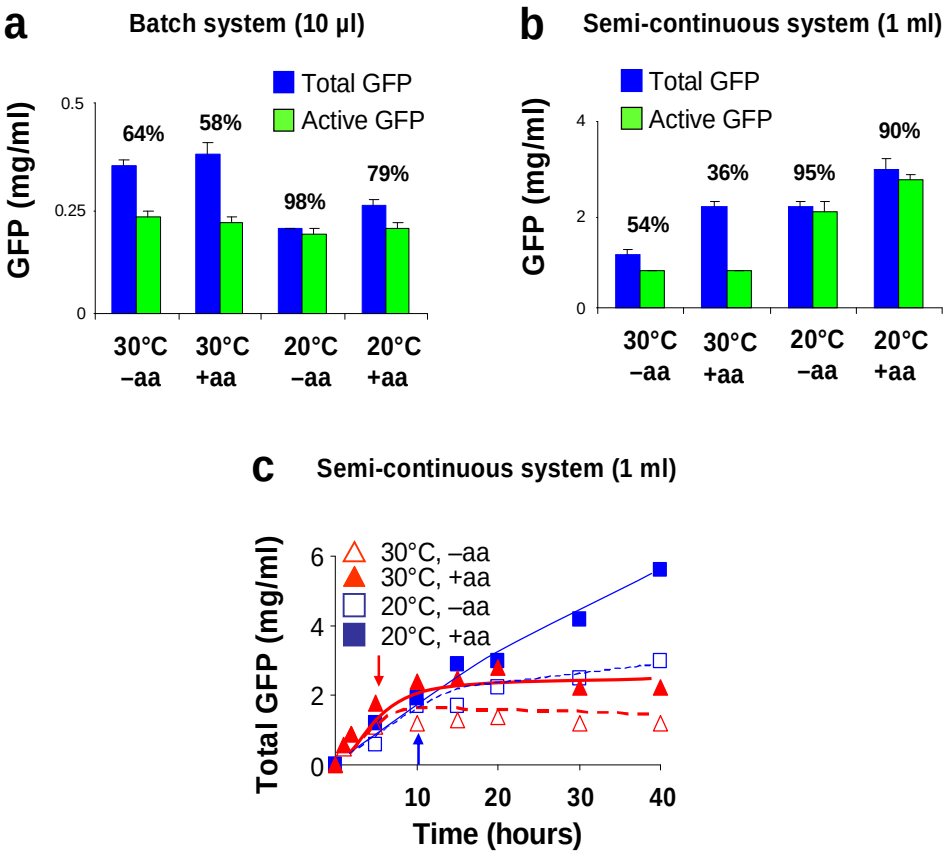

Figure 11: GFP synthesis at 30 and 20°C with and without a second amino-acid addition. (**A**) batch system (10 µl). Blue bars, total GFP; Green bars, active GFP; %-values above bars. (**B**) synthesis of GFP and active fraction after an incubation of 20 h. (**C**) kinetics of GFP synthesis at 30°C (red triangles) and 20°C (blue squares, thick lines). Closed symbols, amino acid additions (arrows) after 7 and 10 h at 30 and 20°C, respectively. Open symbols, no amino acid addition.

metabolized during the reaction of the cell-free system, examples are cysteine, serine, threonine, glutamine and asparagine (Jewett and Swartz, 2004). Therefore, we added a mixture of all twenty amino acids in the middle of the incubation time. A little increase of total synthesis was observed in the *batch system* upon amino acid addition, whereas the amount of the active GFP remained unchanged (+aa; Figure 11a).

A strikingly different response to a second amino acid addition was seen in the *semi-continuous system* (1 ml reaction volume). At 30°C the total GFP was almost doubled without a concomitant increase of the active GFP thus reducing the active fraction to 36% (Figure 11b). However, the amounts synthesized at 20 °C were a surprise, since they were larger than the corresponding 30°C values with and without a second addition of amino acids (incubation time 20 h), but with an active fraction of 90 to 95%. The best results were obtained with a second addition of amino acids after 10 h at 20 °C incubation (Figure 11: b and c). Kinetic analyses revealed that at 20°C the initial rate of GFP synthesis was slower, but the total amount even exceeded that at 30°C after 15 h incubation reaching values twice as large as the corresponding 30°C values (Figure 11c). A possible reason is that metabolization of amino acids runs faster at 30°C leading to a shortage of amino acids after 10 to 15 h in contrast to the situation at 20°C.

3.2 Optimized poly(U)-dependent poly(Phe) synthesis as a tool for studies of protein synthesis process

Two poly(U)-dependent poly(Phe) synthesis systems have been described with comparable efficiency and accuracy, the polymix system of the Uppsala group (Jelenc and Kurland, 1979) and a more simple Mg^{2+}/NH_4^+ polyamine system (Bartetzko and Nierhaus, 1988); called in the following polyamine system). The latter establishes a more stable post-translocational state (POST state) as indicated by a stable E-site occupation in contrast to a spontaneous release of the E-tRNA within minutes in the polymix system (Semenkov et al., 1996). A stable binding of the E-tRNA is also a feature of native polysomes (Remme et al., 1989).

Here we present an optimized polyamine system concerning energy rich compounds such as GTP, ATP, acetylphosphate (Ac-P) and Mg^{2+} concentration applying the criteria of efficiency and accuracy of poly(Phe) synthesis.

tRNA is charged during poly(U)-dependent poly(Phe) synthesis. As a preliminary experiments we tested expression of poly(Phe) either in the presence of $tRNA^{Phe}$ or $tRNA^{bulk}$, i.e. a mixture of all tRNAs from *E. coli*. Our results shown in the Figure 12 revealed that both $tRNA^{Phe}$ or $tRNA^{bulk}$ give comparable efficiency in the poly(Phe) synthesis of about 180 Phe incorporated statistically per ribosome.

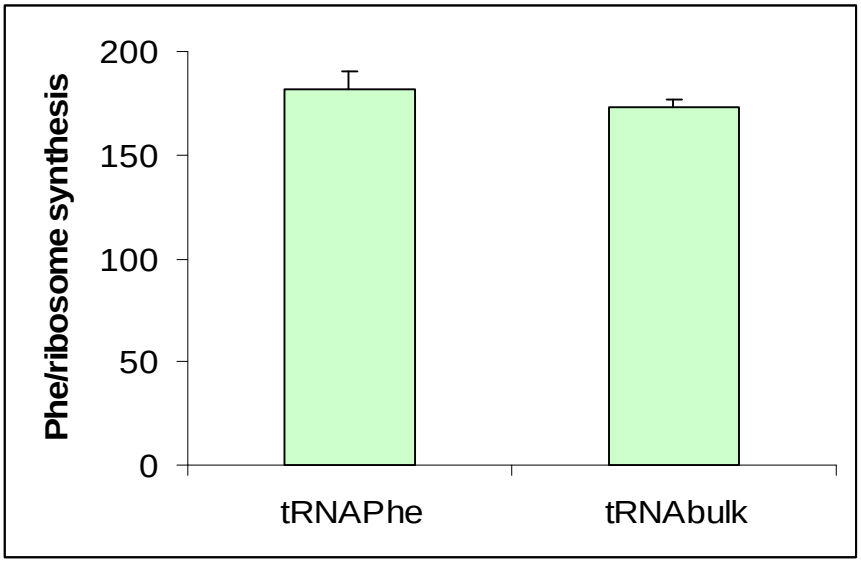

Figure 12: Poly(U)-dependent poly(Phe) synthesis in the presence of $tRNA^{Phe}$ or $tRNA^{bulk}$.

3.2.1 Misreading in the optimized polyamine system

We modified our standard poly(U)-dependent poly(Phe) synthesis to determine misincorporation. ^{14}C-Phe had a low specific activity (10 dpm/pmol) in contrast to non-Phe amino acids labeled with the ^{3}H isotope of high specific activity (about 3000 dpm/pmol). Misincorporation was quantified as incorporation of non-Phe amino acids per 1000 molecules of Phe. Leucine (Leu) is the classical amino acid to be misread in the presence of the codon UUU, since the Leu codon just differs in the wobble position: UUA/G. In order to determine properly a possible misincorporation of Leu and other amino acids, 15 μM $tRNA^{bulk}$ tRNA (similar to the *in vivo* concentration) was added to the standard 2.5 μM $tRNA^{Phe}$. Since the $tRNA^{bulk}$ contains less than 1 μM of a specific tRNA, 10 μM of Leu or another amino acid under observation was added. Such an amount allows saturated charging of the corresponding tRNA, since charging saturation is obtained at a molar stoichiometry of (amino acid):(corresponding tRNA) = (3-5):1 (Rheinberger et al., 1988).

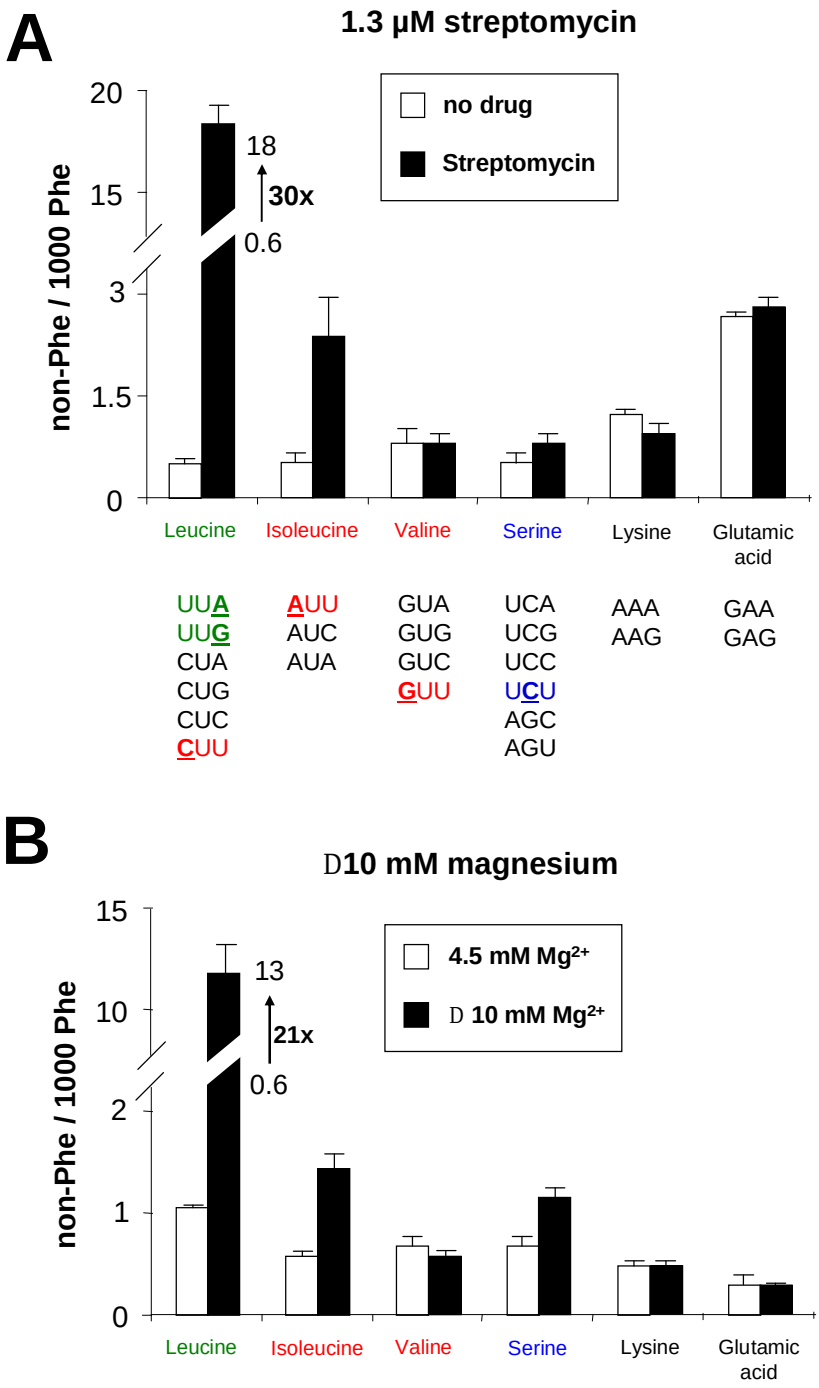

Figure 13: The incorporation of near-cognate and non-cognate aa-tRNAs in the poly(Phe) chain. (**A**) The effect of streptomycin on the aa-tRNAs incorporations. As open bars indicted control reactions where Str was not added. The filled bars represent reactions with 1.3 µM Str. With numbers on the graph showed the factor of increased between non-drug situation and drug situation (increased of the factor of 30). At the bottom of the graph showed the codons sequences correspond to the amino acids. The green codon represents near-cognate tRNA which have mismatch at the third nucleotide position, the red and blue ones are non-cognate with mismatch at the first and the second positions, respectively. (**B**) The effect of Mg^{2+} on aa-tRNAs incorporations. Descriptions like for A.

We define the terms cognate, near-cognate and non-cognate functionally as seen in the respective GTP consumption for incorporation: incorporation of the cognate amino acid (complementary anticodon of the A-site codon) consumes one or two GTPs, that of near-cognate six or more GTPs and non-cognate non (Weijland and Parmeggiani, 1993).

Figure 13 shows the misreading of all near-cognate amino acids using the above definition of near-cognate (green) plus some non-cognate amino acids (red). None of the misreading amino acids with the exception of Leu, the codon of which differs at the wobble position, are misread to any detectable level in the 4.5 polyamine system. In order to study misreading in more detail, we amplified the misreading by two different means: (i) the addition of 1.3 μM streptomycin provoking a 30-fold increase of Leu incorporation (Figure 13a), and (ii) the raise of the Mg^{2+} concentration by 10 mM from 4.5 to 14.5 increasing the Leu incorporation 25-fold (Figure 13b). The figure shows that in no case a mis-incorporation of any amino acid except Leu was increased above the background incorporation, with the questionable exceptions of Ile and Ser.

3.3 Studies on the prokaryotic translation inhibitors

3.3.1 Kasugamycin

3.3.1.1 The impact of Ksg on the growth rate of *E. coli* and formation of 61S ribosomes

The aminoglycoside antibiotic kasugamycin (Ksg) is known to inhibit protein synthesis in eukaryotic and prokaryotic cells. Unexpected from the known effects of the antibiotic exerted *in vitro*, Isabella Moll and coworkers have observed an accumulation of stable ~61S ribosomal particles upon Ksg treatment of the *E. coli* cells *in vivo* (personal communication). These particles consist of an intact 50S subunit, whereas several proteins of the small ribosomal subunit are lacking. They have gained *in vivo* as well as *in vitro* evidence, that these Ksg-particles are capable of translating leaderless mRNAs. Therefore, these 61S-particles could represent an intermediate step in the evolution of ribosomes before the kingdoms had diverged. Thus, the elucidation of the nature of the ribosomal particles formed

in the presence of Ksg might allow new insights in the evolution of the translational machinery.

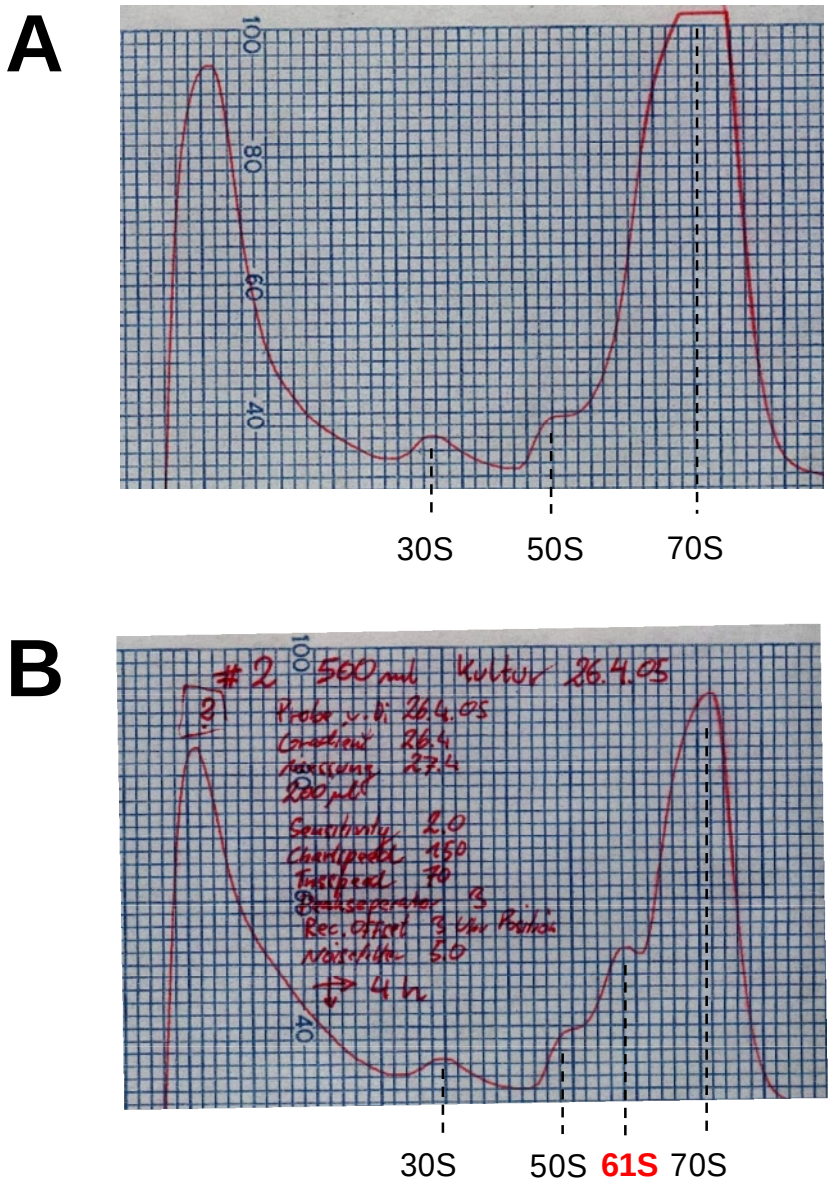

Figure 14: The plot of 70S ribosomal profiles. (**A**) Cells grown in the absence of kasugamycin, indicated associated 70S ribosomes and dissociated 30S and 70S. (**B**) Cells grown in the presence of 200 µM Ksg. Additionally to profile A, the 61S particle can be seen in red.

Together with Isabella Moll from the Institute of Microbiology and Genetics, Vienna Biocenter, Austria we tried to isolate 61S particles from MRE600 or CAN20 cell grown in 100L fermentor. Unfortunately, all our optimizations have failed – we could not observe 61S particles on the analytical sucrose gradient centrifugation.

We checked various parameters, such as time of incubation, time of Ksg addition, capacity of LB medium, oxygen allowance; but we could not observe 61S ribosomal particles. Surprisingly, the same experiments performed by myself in the lab of Isabella Moll revealed evidence for the presence of 61S particles (Figure 14). Unfortunately, any attempts in the MPI for Molecular Genetics failed, even with the samples brought from Vienna to Berlin that have shown a shoulder of 61S particles in Vienna but failed so, when the same sister-samples were re-analyzed in Berlin (Figure 15).

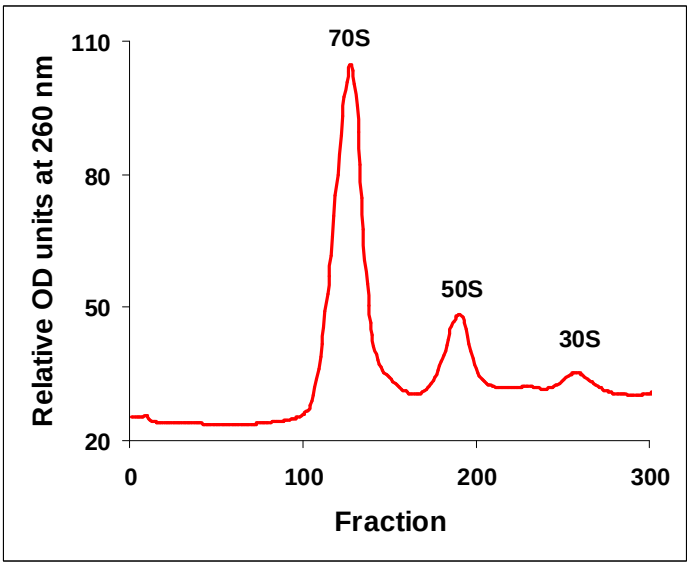

Figure 15: Second sucrose profile made in Berlin from a sample aliquot corresponding to the Sucrose run shown in Figure 14b.

We tested Ksg in RTS system, where we determined the inhibition level and Ksg effect on the accuracy of protein synthesis. Figure 16a shows that specific inhibition in RTS system is less then seen with others antibiotics (compare with Figure 19 and Figure 20b) in contrast to *in vivo* cell growth, where the effect is much more outspoken (Figure 16b). Interestingly, Ksg being related with aminoglycosides, does not impact on the translation accuracy (Figure 16a). Possible explanation for the strong *in vivo* growth inhibition is shown in the Figure 16c. The ribosomal profiles made from the ribosomes isolated from ksg-treated cells documented primary inhibition effect of the 30S assembly by the disappearance of the peak corresponds to 30S, normal 50S peak and reduced 70S peak.

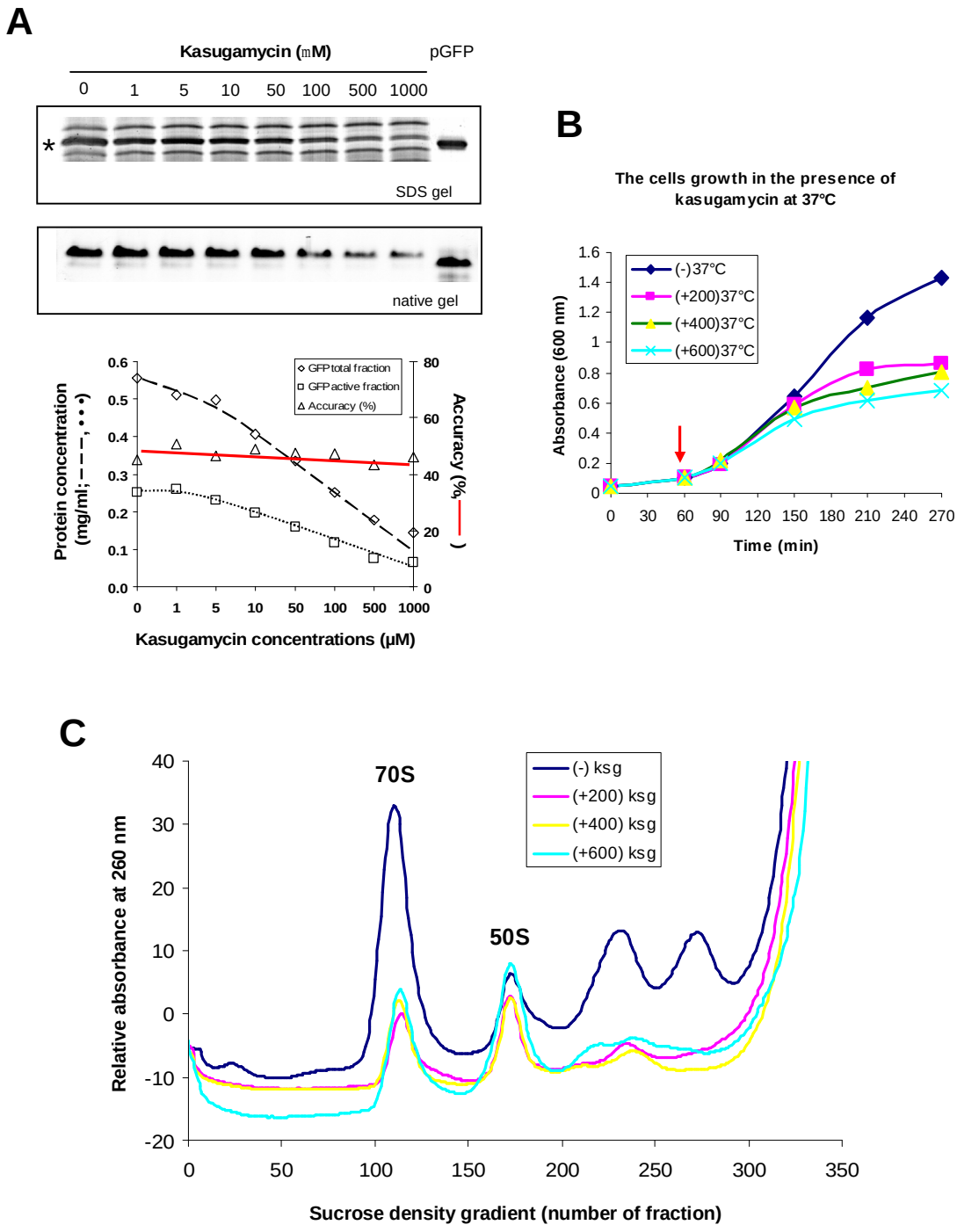

Figure 16: Kasugamycin effect on inhibition of protein synthesis and on inhibition of 30S subunit. (**A**) GFP expression in RTS system with increasing concentration of Ksg visualized by SDS and native PAGE; as a star (*) indicated GFP band; pGFP – pure GFP with known concentration. (**B**) The growth curve of bacteria cell in the presence of three concentrations of Ksg, pink line 200 mg/ml (460 μM), green line 400 mg/ml (920 μM) and blue line 600 mg/ml (1380 μM), the arrow shows the moment of Ksg addition to the cells medium. (**C**) Ribosomal profiled from the cells incubated with different concentrations of Ksg (for concentrations see B).

3.3.1.2 Inhibition of P-site tRNA binding by Ksg *via* mRNA destabilization

To investigate whether Ksg inhibits binding of initiator tRNA *via* perturbation of the mRNA, we extended the experiments of Poldermans and co-workers (Poldermans et al., 1979) to test the effect of Ksg on different types of mRNA.

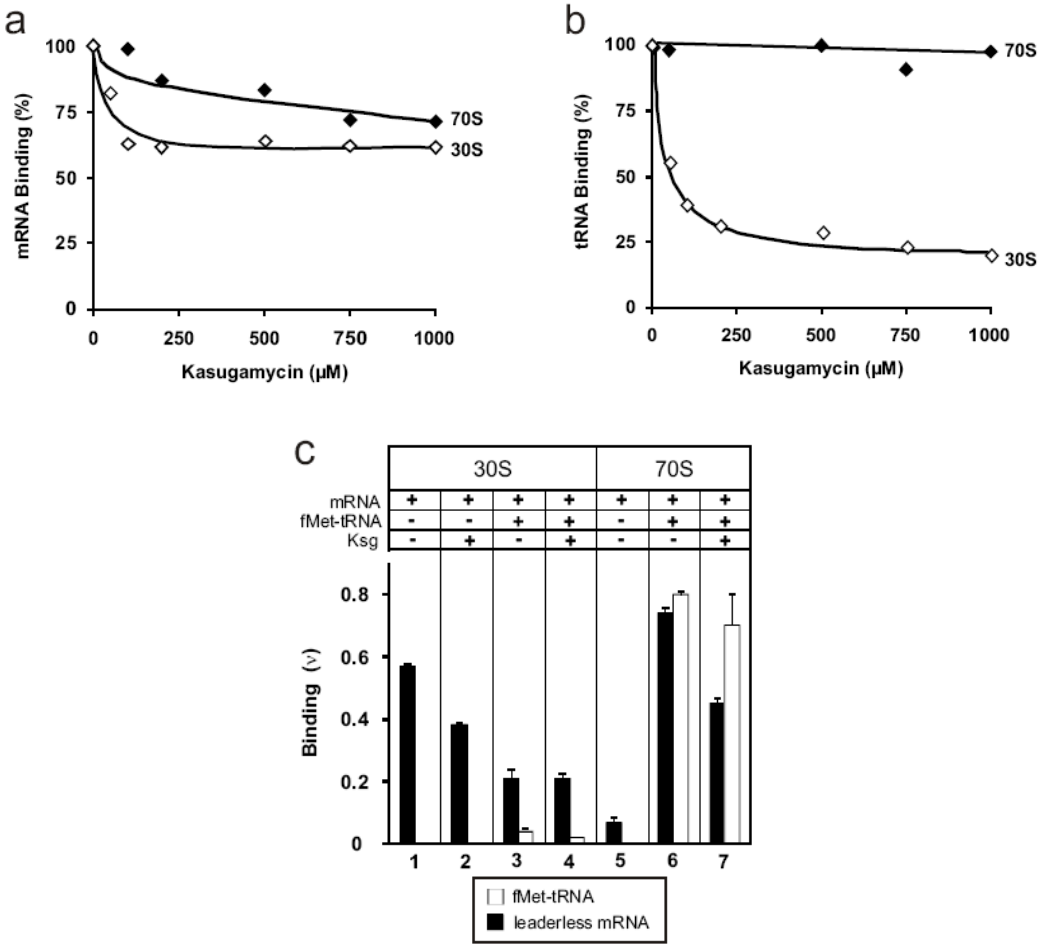

Figure 17: mRNA and tRNA binding to the 30S and 70S in the presence of Ksg

(**a**) The binding of [^{32}P]-labeled mRNA to 30S subunits (open diamonds) and 70S ribosomes (closed diamonds) was measured in the presence of increasing concentrations of kasugamycin (up to 1000 µM). Binding of 100% was assigned to that measured in the absence of the drug (0.62 and 0.67 per 30S and 70S particle, respectively).

(**b**) The binding of [^{14}C]-labeled fMet-tRNA to 30S subunits (open diamonds) and 70S ribosomes (closed diamonds) was measured in the presence of increasing concentrations of kasugamycin (up to 1000 µM). Binding of 100% was assigned to that measured in the absence of the drug (0.14 and 0.51 per 30S and 70S particle, respectively).

(**c**) The binding of a leaderless [^{32}P]-labeled mRNA and/or [^{14}C]-labeled fMet-tRNA to 30S subunits (column 1-4) and 70S ribosomes (column 5-7) was determined in the presence or absence of 500 µM kasugamycin (Ksg). Binding is given as pmols of leaderless mRNA (white bars) or fMet-tRNA (black bars) per pmol of 30S or 70S. The error bars indicate the standard error from the mean for three independent experiments.

[^{32}P]-labeled MVF-mRNA and f[^{3}H]Met-tRNA were incubated together with the 30S subunit or the 70S ribosome and their binding measured in presence of increasing concentrations of Ksg. As can be seen in Figure 17a, the binding of the MVF-mRNA to the ribosome in the presence of fMet-tRNA was slightly inhibited (25%) by Ksg on 70S ribosomes and more strongly inhibited on 30S subunits (40%). However, more dramatic was the specific inhibition of binding of initiator fMet-tRNA to 30S subunits in the presence of MVF-mRNA (up to 75 % inhibition), whereas binding to 70S ribosomes remained unaffected (Figure 17b). We observed similar results regardless of whether Ksg was preincubated with the ribosomal particles before addition of mRNA and tRNA, or whether Ksg was added prior to initiation complex formation (data not shown). Furthermore, the effect on mRNA binding was less dramatic when the mRNA contained a strong Shine-Dalgarno (SD) sequence (data not shown). In light of our structural data, this result suggests that the additional basepairing between the SD-antiSD enables the mRNA to be more stably bound to the ribosome, even in the presence of Ksg.

In contrast to translation initiation of canonical mRNAs, translation of leaderless mRNAs *in vivo* has been reported to be unaffected by Ksg (Chin et al., 1993), (Moll and Bläsi, 2002). Therefore, we were interested in examining *in vitro* the effect of Ksg on binding of leaderless mRNA and fMet-tRNA to 30S subunits and 70S ribosomes. Figure 17c reveals that in the absence of fMet-tRNA, the binding of leaderless mRNA was strikingly better to 30S subunits (0.57 per 30S, column 1) than to 70S ribosomes (0.07 per 70S, column 5) and that the addition of 500 µM Ksg produced only a modest inhibition (25%) of binding of the leaderless mRNA to the 30S subunits (column 2). In the presence of fMet-tRNA, the trend was exactly opposite, such that the binding of both leaderless mRNA and fMet-tRNA to 30S subunits was very poor (0.2 and 0.04, respectively, column 3), whereas binding of both to 70S ribosomes was extremely efficient (0.7 and 0.8, respectively; column 6). This suggests that leaderless mRNAs form a very stable complex with fMet-tRNA on 70S ribosomes, but that this complex is very unstable on 30S subunits and results in dissociation of the fMet-tRNA and mRNA during filtration. In addition, the presence of high concentrations of Ksg (500 µM Ksg) produced only a modest inhibition (29%) on binding of leaderless mRNA to 70S ribosomes and had even less influence (13%) on fMet-tRNA binding (column 7).

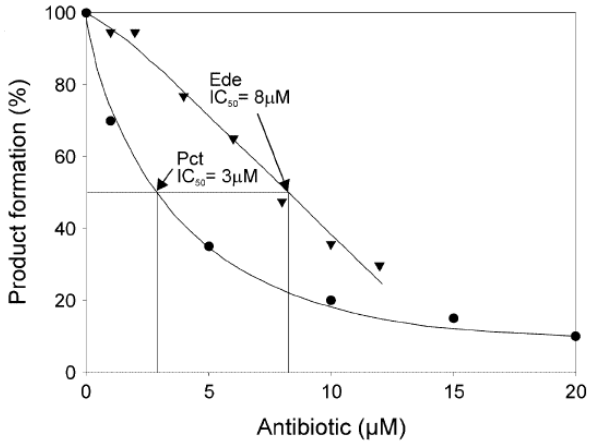

Figure 18: Effect of Ede and Pct on coupled transcription-translation system. Coupled *in vitro* transcription-translation was performed in the presence of increasing concentrations of edeine (,) and pactamycin (**I**). The relative amount of GFP protein product formed is given as percentages, where 100% is arbitrarily assigned as the product formed in the absence of antibiotic. The inset shows a measure of the translation fidelity in the presence of edeine and pactamycin (open symbols).

This demonstrates that initiation complexes formed between leaderless mRNA and fMet-tRNA on 70S ribosomes are resistant to Ksg action, consistent with the *in vivo* data (Chin et al., 1993; Moll and Bläsi, 2002). On the 30S subunit, the already low binding of the fMet-tRNA and leaderless mRNA precluded a dramatic affect being observed upon addition of Ksg, however the binding of fMet-tRNA was reproducibly decreased (column 4).

3.3.2 Edeine and Pactamycin and their influence on translation accuracy

The most physiological *in vitro* system for protein synthesis currently available is the coupled transcription-translation system. We utilized this system for the expression of green fluorescence protein (GFP) gene in order to define the concentration window, where Ede and Pct block protein synthesis (for GFP expression and optimization of coupled transcription-translation system see section 3.1. In the Figure 18, it can be seen that half-inhibitory concentrations (IC_{50}) of Ede and Pct were ~8 µM and ~3 µM, respectively, and that 80% inhibition was seen at concentrations >12.5 µM.

The synthesized GFP was measured both in SDS and native gels, the former assessing the total amount of synthesized protein whereas the latter enabled the determination of the fluorescence in the gel and thus reflects the fully folded, active amount of GFP. The expectation is that a drug inducing misincorporations will reduce the active fraction more strongly then the total synthesis, so that the ration (active fraction)/(total synthesis) will decrease with the increasing drug concentration. In contrast, if a drug does not affect the decoding

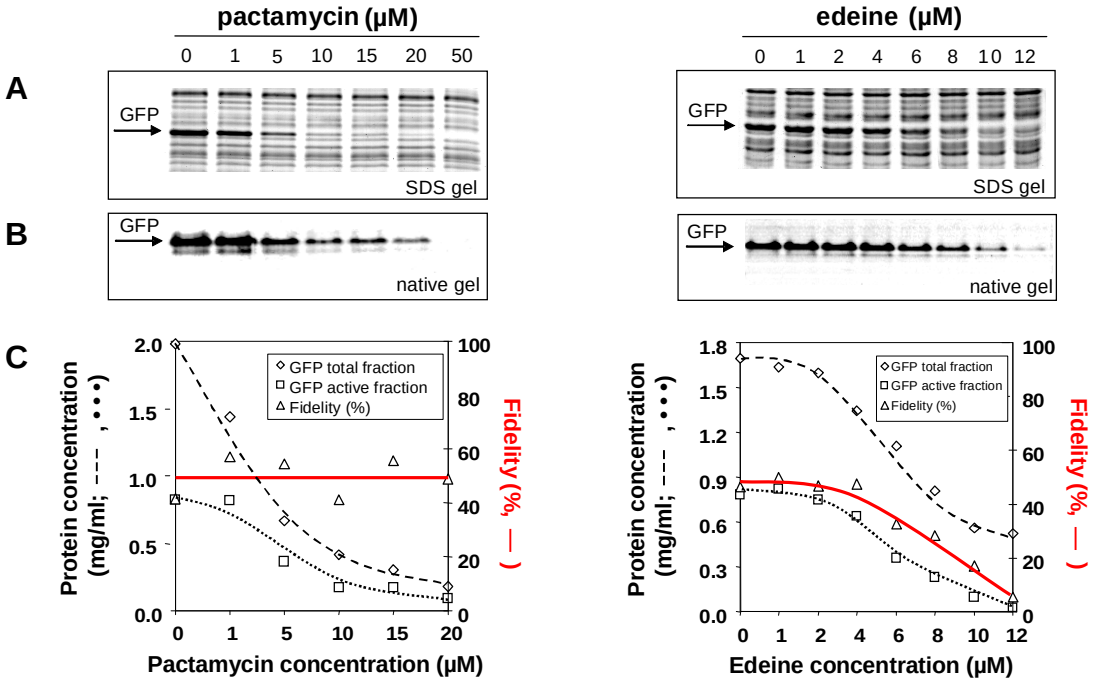

Figure 19: Effect of edeine and pactamycin on translational fidelity in an *in vitro* transcription-translation system

(A) 1.5 µl aliquots from GFP samples expressed in the coupled transcription/translation system were applied to 15% SDS-PAGE GFP protein with increasing concentrations of pactamycin (left, 0-50µM) or edeine (right, 0-12µM). The position of the GFP protein is indicated by an arrow in each gel (27 kDa). The gels were stained by Coomassie Brilliant Blue R-250.

(B) 1.5 µl aliquots from the identical samples used in (A) were subjected to electrophoresis in a native 15% gel and the fluorescence band in the non-stained gel was determined using the FluorImager 575 from Molecular Dynamics.

(C) Graphical representation showing the total (¯) and active (*) amounts of GFP produced (mg/ml) for the samples as in (A). The ratio of active GFP to total GFP protein provides a measure of the translational fidelity (dark lines with r symbols) as is given as a percentage, where a translational fidelity of 100% is arbitrarily assigned to a ratio (active fraction)/(total synthesis) observed with the GFP control kindly provided by Roche.

accuracy, the active amount and total amount of synthesized protein (GFP) will decreased proportionally and accordingly the ratio (active fraction)/(total synthesis) will not change with increasing drug concentration.

The expectation was verified with streptomycin, the classical inducer of misreading, and thiostrepton, which does not affect the decoding accuracy. Therefore, this method provides a measure of overall misincorporation, a feature of the coupled transcription-translation system that was exploited and demonstrated for the first time. The expression of GFP was measured in the presence of increasing concentrations of Ede and Pct (Figure 19). The total

amount of GFP produced was determined by SDS-PAGE (Figure 19a) and the active GFP amount by measuring of the fluorescence of the GFP on native gels (Figure 19b). As described above, the ratio of the active GFP to the total GFP provides a measure of the translation fidelity of the system. As seen in Figure 19c, the ratio of active to total GFP did not change with increasing Pct concentrations, demonstrating that Pct does not influence the translation fidelity of the system. In contrast, with increasing Ede concentrations, there was dramatic decrease in the ratio of active GFP to total protein, shown in Figure 19c as translation fidelity (solid red line with triangle symbols). It follows that Ede is a strong inducer of misincorporations.

3.3.3 Effects of aminoglycosides and some other antibiotics on protein synthesis in vitro

Here we compare the effects of aminoglycosides and some other antibiotics in

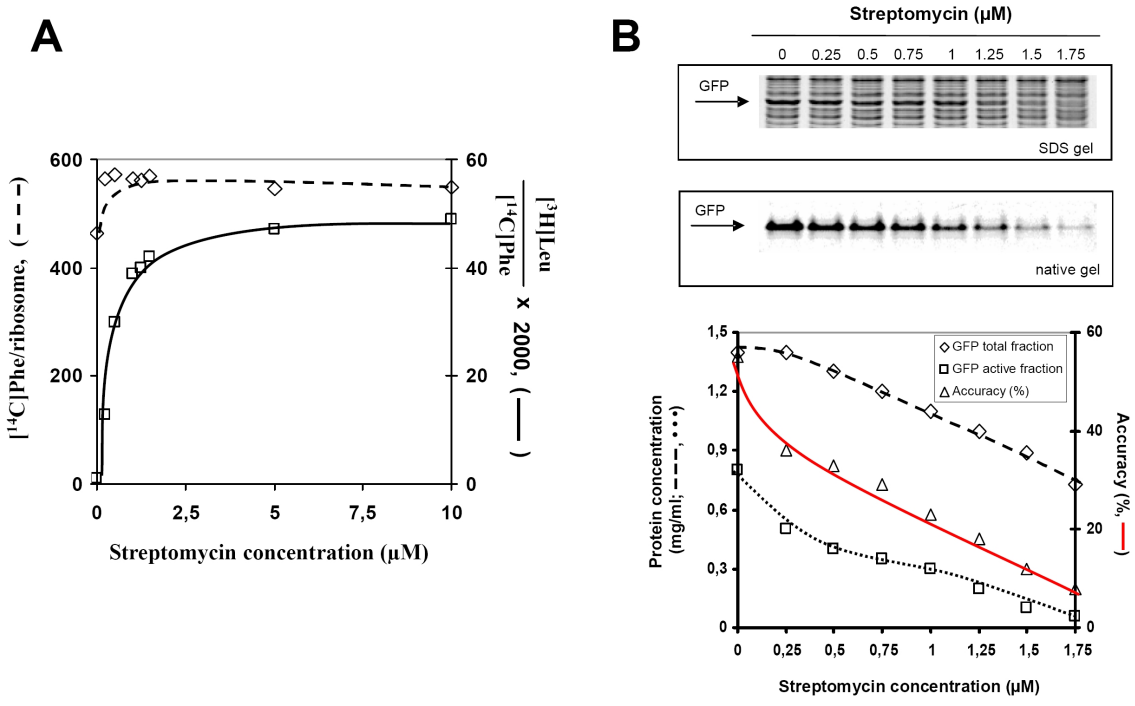

Figure 20: Misincorporations caused by streptomycin measured in both poly(U)-dependent poly(Phe) system and RTS 100. (**A**) Misincorporation measured in the poly(Phe) system *via* Leu incorporation (100xLEU/(Leu+Phe)). The solid line indicates the incorporation of Leu (Leu incorporation per 2000 amino acids) and the dashed line the poly(Phe) synthesis with 200-300 nucleotides on average. (**B**) Expression of GFP in RTS 100 in the presence of Streptomycin. The total expression and active amount was quantified from gels and plotted (total expression - dashed line, active amount - dotted line). The active fraction of GFP is shown as a solid line.

the poly(U)-dependent poly(Phe) synthesis system and a coupled transcription-translation system (RTS 100, Roche). We reported already that two antibiotics pactamycin and the aminoglycoside streptomycin increased the total Phe incorporation almost twice, whereas pactamycin did not (Dinos et al., 2004). Figure 20a shows additional details with streptomycin: Already at the lowest streptomycin concentration of 0.5 µM Phe incorporation was increased by 25 %, whereas Leu misincorporation was maximal at 5 µM and increased about 50-fold starting from 1 Leu incorporated per 2000 Phe in the absence of the drug.

The drug effects were also studied in the coupled transcription-translation system, assessing the active fraction of GFP as (active GFP)/(total GFP)x100 (Figure 20b, see Iskakova et al., 2006 for details). Therefore, the active fraction of

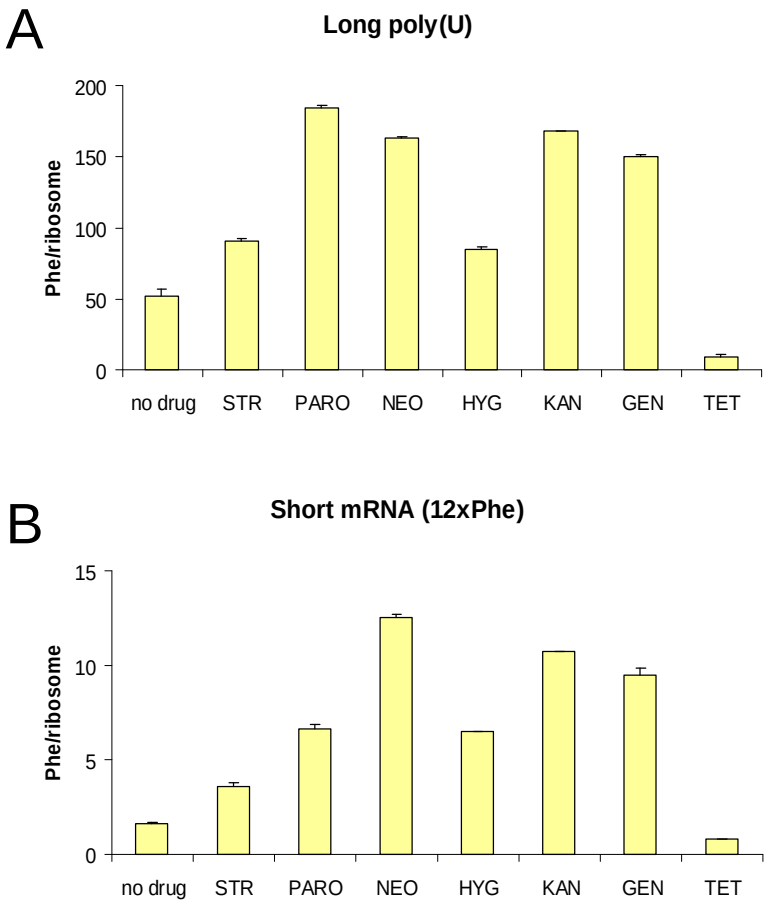

Figure 21: Poly(U)-dependent poly(Phe) synthesis in the presence of aminoglycosides. Antibiotics abbreviations and concentrations as followed: streptomycin (STR, 50 µM), paromomycin (PARO, 50 µM), neomycin (NEO, 50 µM), hygromycin B (HYG, 50 µM), kanamycin (KAN, 50 µM), gentamycin C (GEN, 50 µM), tetracycline (TET, 500 µM). Poly(Phe) synthesis based on (**A**) long poly(U) mRNA and (**B**) short $(UUC)_{12}$ mRNA.

synthesized GFP can be calculated as (active GFP)/(total GFP)x100.

In contrast to the stimulatory effects of streptomycin on poly(U) dependent poly(Phe) synthesis, the drug blocked efficiently GFP synthesis in the coupled system, 50% inhibition already at 1.75 µM, whereas the active GFP was blocked to almost 100 % at this concentration (Figure 20b). This result indicates the

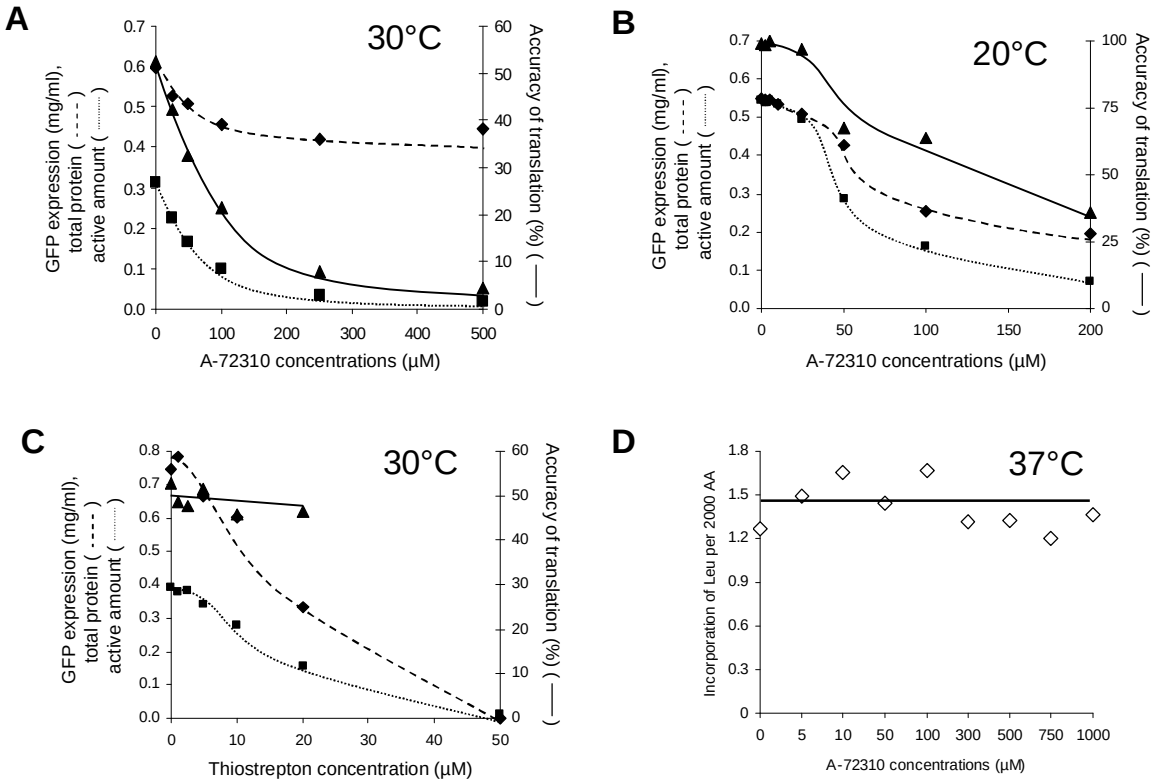

Figure 22: NRI-related impact on RTS reaction and leucine incorporation in poly(U)-dependent poly(Phe) synthesis. (A) Disruption of translation accuracy caused by A-72310 in the reaction temperature of 30°C. As a dashed line indicated total GFP synthesis, and as dotted line the active amount of GFP. The solid line represents the translation fidelity as a ration between active amount and total protein synthesis. (B) Disruption of translation accuracy caused by A-72310 in the reaction temperature of 20°C. Descriptions like for A. (C) Control reaction with thiostrepton (30°C reaction temperature). Descriptions like for A. (D) Leucine incorporation in poly(U)-dependent poly(Phe) synthesis in the presence of increased concentrations of A-72310.

extreme sensitivity of GFP for mis-incorporation, since a slight disorder of the 11 β-barrel structure protecting the fluorescent structure in its middle (Ormo et al., 1996; Yang et al., 1996) allows access of water and oxygen thus quenching the florescent (see Iskakova et al., 2006). Therefore, the GFP-mRNA is excellently suited to test overall misincorporation effects in the presence of a natural mRNA.

One intriguing effect caused by streptomycin and other aminoglycosides is stimulation of poly(Phe) synthesis as mentioned in the upper paragraph. One possibility is that in addition to misreading the aminoglycosides facilitate frameshifts that might enhance recycling of ribosomes and thus explain the increase in Phe incorporation. In order to test this possibility we used the pU-SD mRNA containing twelve Phe codons UUC (see Materials and Methods or Márquez, 2002, page 39) thus not allowing frameshifts anymore. The Phe incorporation was checked in the presence of aminoglycosides. Figure 21 shows that aminoglycosides strongly stimulate synthesis of Phe. Paromomycin, neomycin, kanamycin and gentamycin stimulate poly(Phe) synthesis from long poly(U) three times more than to the control reaction in the absence of drugs. Moreover, expression of poly(Phe) from $(UUC)_{12}$-mRNA is stimulated by aminoglycosides to a similar extent (3-6 times more then in the reaction without drugs) thus excluding frameshift as the reason for the increase of Phe incorporation.

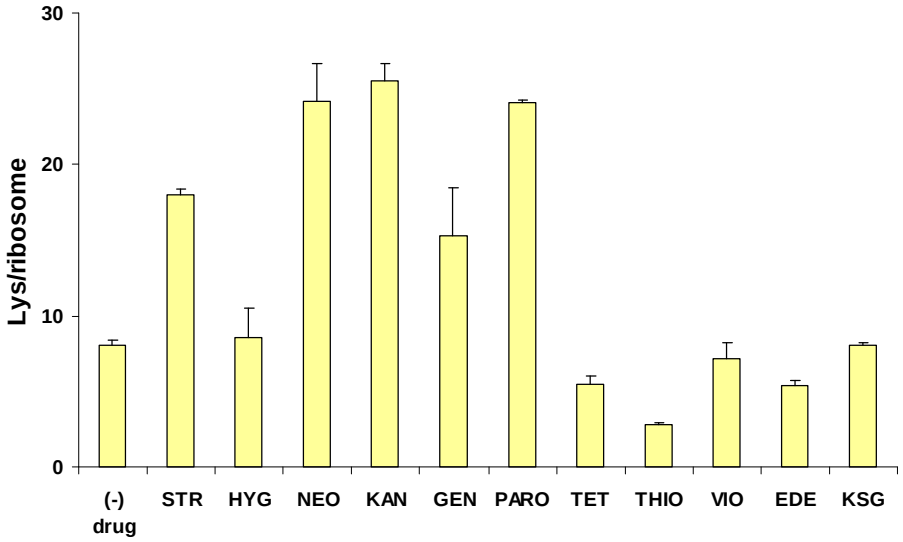

Figure 23: Poly(A)-dependent poly(Lys) synthesis in the presence of aminoglycosides. Antibiotics abbreviations and concentrations as followed: streptomycin (STR, 50 µM), hygromycin B (HYG, 50 µM), neomycin (NEO, 50 µM), kanamycin (KAN, 50 µM), gentamycin C (GEN, 50 µM), paromomycin (PARO, 50 µM), tetracycline (TET, 500 µM), thiostrepton (THIO, 5 µM), viomycin (VIO, 50 µM), edeine (EDE, 50 µM), kasugamycin (KSG, 200 µM).

As control drugs thiostrepton and tetracycline were selected; thiostrepton effects in the RTS are shown in Figure 22c and tetracycline effects on poly(Phe) synthesis is shown in Figure 20. They block both poly(Phe) and GFP synthesis

and do not significantly affect both misreading in the poly(Phe) synthesis and the active fraction of GFP.

To analyze whether or not some aminoglycosides can stimulate protein expression also in the poly(A)-dependent poly(Lys). Figure 23 demonstrates that almost all aminoglycosides except hygromycin B stimulated poly(Lys) synthesis in contrast to control drugs which do not affected poly(Lys) synthesis or impaired it. This finding is in striking contrast to the translation of natural mRNA, for example that of GFP (Figure 20). Aminoglycosides stimulate also the Phe incorporation depending of a short mRNA with 12 UUC codons (Figure 21b). This finding indicates that the stimulation is not related to frameshifts, but possibly caused by a loosely bound mRNA, since the number of incorporated Phe per ribosome exceeded the number of codons per mRNA.

3.3.4 Novel Ribosomal Inhibitor (NRI)

An interesting and until now unique response concerning misreading and active fraction of GFP was observed with the new drug Novel Ribosomal Inhibitor (NRI, A-72310) of the naphthyridine class. This drug shows a very strong effect on the active fraction of GFP, but in striking contrast no effect on misreading in the poly(Phe) synthesis (Figure 22 a and b *versus* c). Since the total GFP synthesis is only moderately reduced by maximally 30% (from 0.6 to 0.4 mg/ml) indicating that errors such as frameshifting or processivity effects do not play a role, we conclude that this drug is a strong misreading inducing drug at some codons, but not with UUU. This surprising finding might represent the until now elusive inhibition mechanism of this drug (Shen et al., 2005).

Additionally we tested whether NRI influences the charging of $tRNA^{Phe}$ but we could not observe any effect (Figure 24).

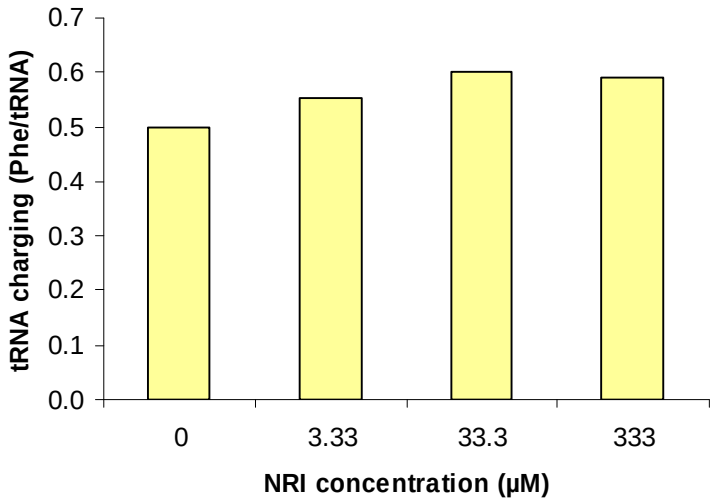

Figure 24: tRNA^{Phe} charging in the presence of various concentrations of NRI (A-72310)

3.3.5 Effects of aminoglycosides and control drugs in single reactions of the elongation cycle under optimal conditions

The allosteric three site model predicts the existence of two types of the A-site occupation: an initiation type (i-type), when only one tRNA is bound to the ribosome, i.e. P-site tRNA, and an elongation type (e-type), when two tRNAs are at P- and E-site (Rheinberger and Nierhaus, 1986).

Indeed, Hauser has demonstrated that occupation of the A-site could not be blocked by aminoglycosides, when only one tRNA was present at the P-site (i-type), whereas a total blockage was observed when tRNAs were present at the P and E-sites. We wanted to repeat the results of Hausner, but here with heteropolymeric mRNA, since the results of Hausner were performed with poly(U), and having the same codon in A and E sites is not free of ambiguities. In order to relief this ambiguity we decided to perform corresponding experiments but in the presence of heteropolymeric mRNA after establishing a POST state *via* canonical, EF-G dependent translocation leaving EF-G in the mixture to which the drugs were added. Figure 25 demonstrates disappointing effect, that the aminoglycosides do not block the A-site occupation of the e-type under these conditions. Therefore we decided to repeat the Hausner experiments but now not only in the presence of poly(U) mRNA but also in the presence of heteropolymeric MFV mRNA. The special point of the Hausner experiments was that the E-site was not occupied *via*

translocation reaction, but rather by simply binding cognate tRNA to the E-site by adding four molar excess over ribosome to the mixture. The results are presented in the Figure 26A and B. Indeed the poly(U) experiment reproduced the Hausner results in a perfect manner, i.e. aminoglycosides blocked the A-site occupation stronger than the standard blocker tetracycline. In striking contrast, the addition of $tRNA_f^{Met}$ to the E-site in the MFV-mRNA programmed ribosomes (Figure 26B) showed only a marginal effect concerning A-site blockage.

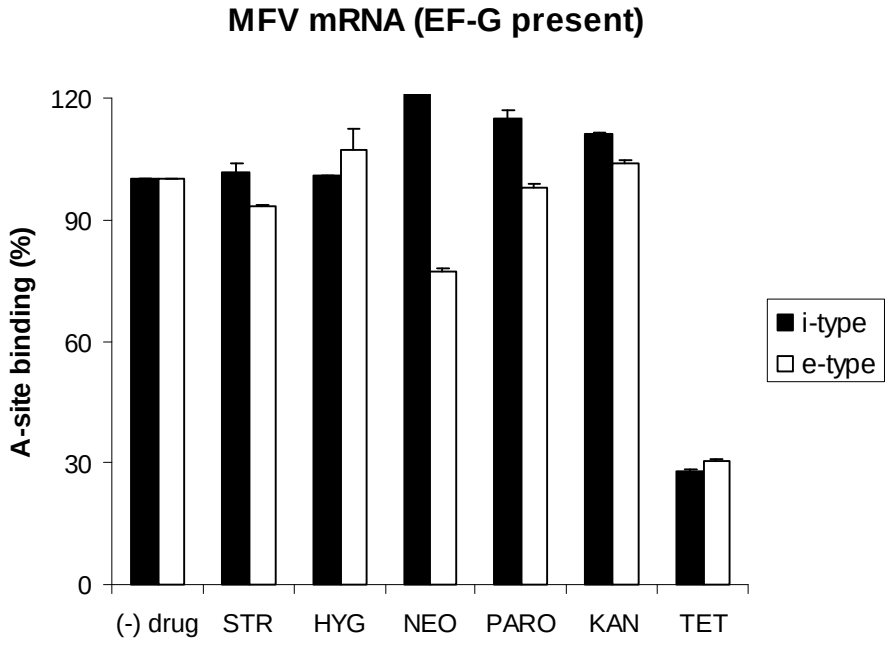

Figure 25: The two types of tRNA binding to the A-site in the presence of aminoglycosides and EF-G. 100% binding of i-type and e-type are equal to ν=0.45 and ν=0.49, respectively. The concentrations and abbreviations of antibiotics are as followed: streptomycin (STR, 50 μM), hygromycin B (HYG, 50 μM), neomycin (NEO, 50 μM), paromomycin (PARO, 50 μM), kanamycin (KAN, 50 μM) and tetracycline (TET, 500 μM).

In the final experiment we asked whether a POST state established in the canonical way *via* EF-G dependent translocation and after subsequent removal of EF-G showed also an aminoglycoside effect on the A-site occupation. These experimental set-up is related to recent published report by Frederick and colleagues, who challenged the aminoglycoside effects of the Hausner experiments by showing that the aminoglycosides could trigger a back-translocation (Shoji et al., 2006). Such a back-translocation is only possible with

the POST state but not with the P_i state, probably provoking the Hausner results.

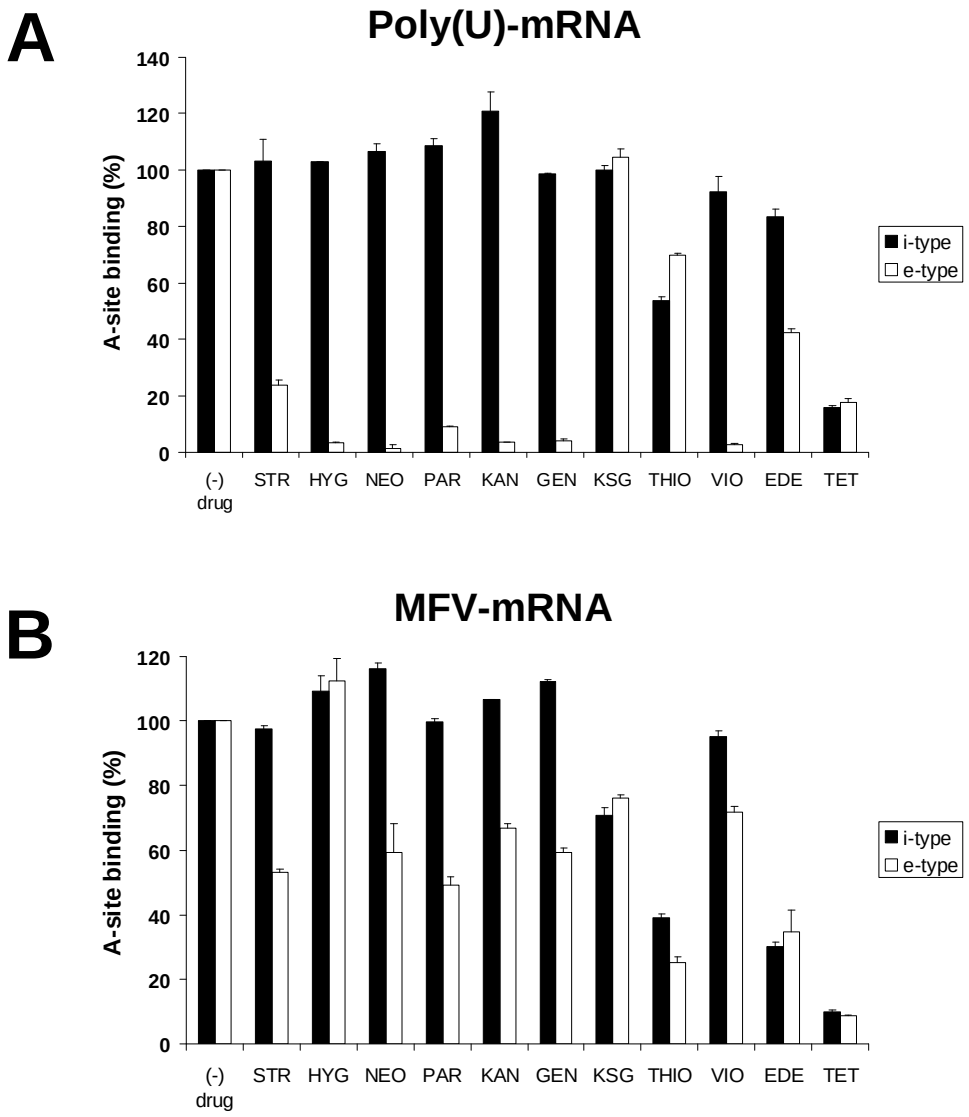

Figure 26: i-type and e-type binding of the tRNA to the ribosomal A-site.

(A) A-site binding with poly(U)-mRNA-programmed 70S ribosome, (-) drug – control reaction without antibiotics (ν=0.17, 100%)
(B) A-site binding with MFV-mRNA-programmed 70S ribosome, (-) drug – control reaction without antibiotics (ν=0.12, 100%)
The concentrations and abbreviations of antibiotics are as followed: streptomycin (STR, 50 μM), hygromycin B (HYG, 50 μM), neomycin (NEO, 50 μM), paromomycin (PARO, 50 μM), kanamycin (KAN, 50 μM) and gentamycin (GEN, 50 μM), kasugamycin (KSG, 200 μM), viomycin (VIO, 50 μM), edeine A (EDE, 50 μM), tetracycline (TET, 500 μM).

However we showed already above that standard POST state in the presence of EF-G does not show any A-site inhibition. A possible reason could be that these experiments were performed in the presence of EF-G and GTP that could stabilize

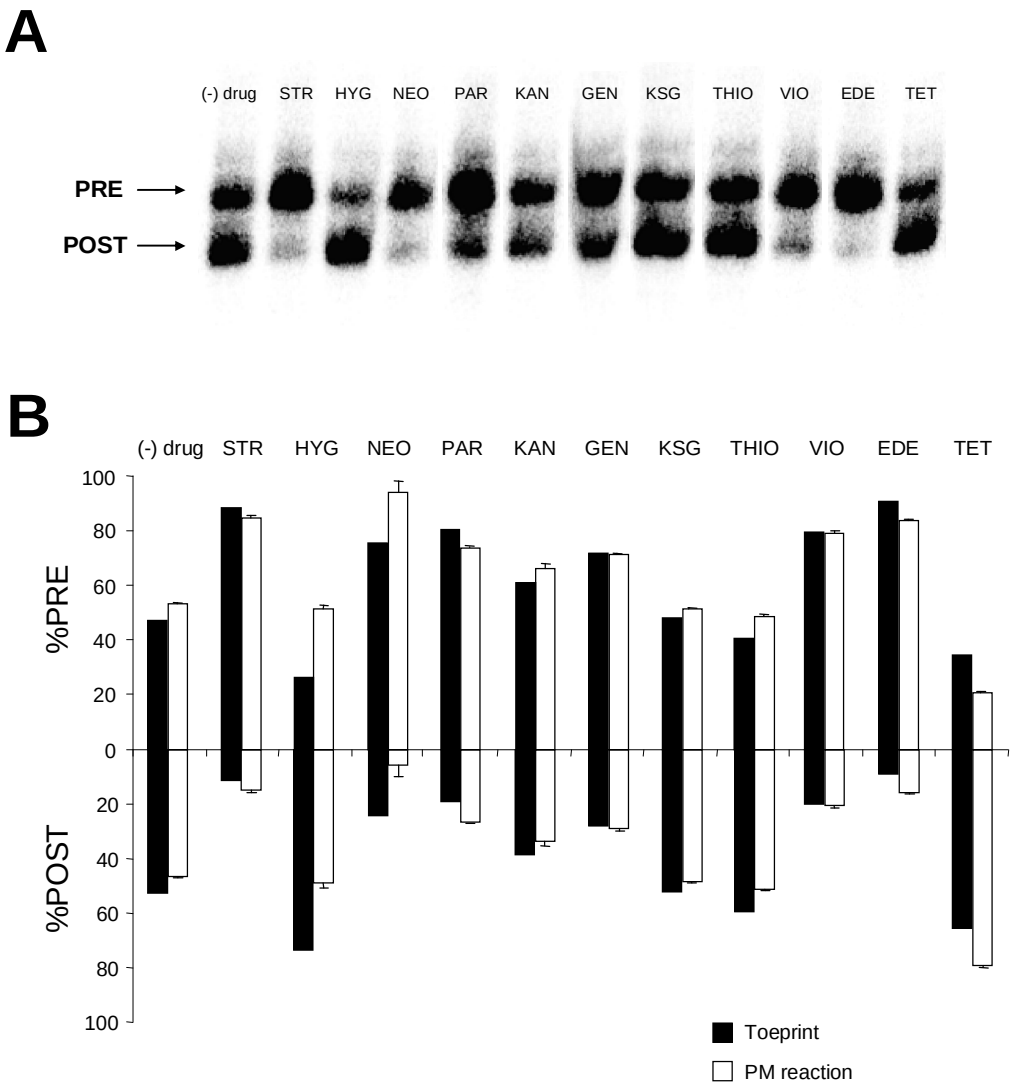

Figure 27: The impact of Aminoglycosides and control drugs for a back-translocation action. The POST state was achieved via EF-G dependent translocation, after this EF-G had been removed via pelleting through a 10% sucrose cushion (for details see Material and Methods, section 2.2.23, page 69) The antibiotic concentrations and abbreviations like described in the legend of Figure 26 (**A**) Radiogram of toeprint assay. PRE state is equal to transcription stop at +16, and POST state is equal to stop at +19. (**B**) Quantification of toe print radiogram as a percent of PRE and POST ribosomes in the solution in the presence of drug and puromycin reaction quantified as a PRE and POST ribosomes in the presence of drug.

the POST state, whereas Frederick and colleagues constructed a POST state in the absence of EF-G. Therefore, we test in the next experiment, whether or not we can reproduce the results of Frederick and colleagues using an isolated POST state free of EF-G shows. In parallel, we controlled the presence of the POST state by both the puromycin reaction and tRNA binding as well as monitored the ribosome location on the mRNA with toeprinting assays on the other (Figure 27).

The results were consistent in both techniques, i.e. the puromycin reaction was abolished when the toeprinting assay revealed a back-translocation demonstrating convincingly a back-translocation of the tRNAs. These results reproduce those of Frederick. Furthermore, our data clearly indicate that in the presence of EF-G and GTP as *in vivo* the back-translocation induced by aminoglycosides is not relevant and cannot explain the bactericidal effect of these antibiotics.